

PHASE TRANSFORMATION MONOCLINIC-TETRAGONAL OF ZrO_2 NANOPARTICLES BY DOPING OF METAL ION VIA THE SIMPLE PRECIPITATION PROCESS

¹K. Anandan, ²V. Rajendran

¹Assistant Professor, Department of Physics, AMET University, Chennai 603 112, Tamilnadu, India

²Associate Professor, Department of Physics, Presidency College, Chennai 600 005, Tamilnadu, India

Abstract : Pure and Co-doped ZrO_2 nanoparticles were successfully synthesized by the simple precipitation process. The synthesized samples were characterized by X-ray diffraction (XRD), Fourier transform infrared (FTIR) spectroscopy, Ultraviolet-visible (UV-vis) spectroscopy and Photoluminescence (PL) emission spectroscopy techniques. The structural and optical properties of the pure and Co-doped ZrO_2 were comparatively discussed.

Keywords: ZrO_2 ; Co-doped; Nanoparticles; Structural properties; Optical properties

I. INTRODUCTION

Nanomaterials are defined as those materials whose length scale lies within the nanometric range, i.e. from one to a hundred nanometers. Within this length scale, the properties of matter are considerably different from the individual atoms, molecules and bulk materials. The physical, chemical, electrical and optical properties of these materials are size and shape dependent and they often exhibit important differences in the bulk properties. Currently, the importance of nanomaterials in the field of luminescence has been increased, especially; the metal oxide nanomaterials as they exhibit enhanced optical and structural properties. Among the metal oxides, zirconia (ZrO_2) is one of the most well studied transition metal oxide and it is a widely utilized material which finds application in numerous fields such as high-performance ceramics, catalysts, sensors and optical fields [1–3]. Moreover, zirconia is a widely used inorganic material which is chemically stable, non-toxic, and not dissolvable in water. Thus it could be an attractive candidate for drinking water purification.

Zirconia displays three polymorphs at atmospheric pressure: at low temperatures the monoclinic $C_{2h}^{5_{2h}}$ phase (~space group $P2_1/c$), above 1400 K the tetragonal $D_{4h}^{15_{4h}}$ ($P4_2/nmc$) phase, and above 2600 K the cubic fluorite O_h^5 ($Fm3m$) phase [4]. Both the monoclinic and tetragonal phases can be obtained by distortion of the simple cubic structure. In general, at room temperature crystalline zirconia (ZrO_2) exists in the monoclinic phase; however, the tetragonal phase can be stabilized by the addition of substitutional cations. The stabilized zirconia has been extensively studied both theoretically and experimentally due to its wide technological applications [5, 6].

Several methods have been adopted for the preparation of ultrafine zirconia nanoparticles, among the methods; precipitation method is widely adopted in laboratories because of its low preparation cost and simple process. The present investigation deals with pure and metal ion doped ZrO_2 nanoparticles by the chemical precipitation method and their structural and optical property was also studied.

II. EXPERIMENTAL PROCEDURE

Materials

The zirconium nitrate ($ZrO(NO_3)_2 \cdot xH_2O$, purity 99.9 %), sodium hydroxide (NaOH, purity 99 %), Cobalt (II) chloride hexahydrate ($CoCl_2 \cdot 6H_2O$, purity 99 %) and distilled water used in this work were analytical grade reagents, without any further purification.

Synthesis of pure and Co doped ZrO_2 nanoparticles

Pure and Co doped ZrO_2 samples were synthesized by the simple precipitation process, and all the chemicals used in this work were analytical grade reagents, without any further purification. In a typical process, 0.3 M of zirconium nitrate ($ZrO(NO_3)_2 \cdot xH_2O$) was dissolved in 100 ml aqueous medium under vigorous stirring. A light yellowish precipitate was obtained by the addition of sufficient amount of NaOH to the above transparent solution. The resultant precipitate was washed with distilled water and absolute ethanol to remove the impurities and dried at 120°C for 12 hrs. Finally, it was calcined at 450°C for 2 hrs to obtain the ZrO_2 samples. In the same way, Co-doped ZrO_2 sample was prepared with the addition of 1 mol % cobalt chloride ($CoCl_2$). Prepared powder was characterized by different techniques to get a complete understanding of its particle size, crystallographic phases and optical properties of zirconium oxide.

Characterization of the samples by different techniques

The crystalline size and structures of the samples were characterized by X-ray diffraction on a rotating-target X-ray diffractometer (JSD-DEBYFLEX 2002) equipped with monochromatic high intensity $CuK\alpha_1$ radiation ($\lambda = 0.15406$ nm, 40 kV, 100 mA). The samples were scanned in the range of 20 to 70° (2 θ), with a scanning rate of 0.005°/s and step size of 0.02°. The functional groups of the samples were recorded by FTIR spectroscopy on the Nicolet 205 spectrometer in the range of 4000 – 400 cm^{-1} . The optical absorption spectra of the samples were obtained from a Varian Cary 5E spectrophotometer in the range of 200–800 nm. The photoluminescence emission spectra were carried out on a Fluoromax-4 spectrofluorometer with an Xe lamp as the excitation light source.

III. RESULTS AND DISCUSSION

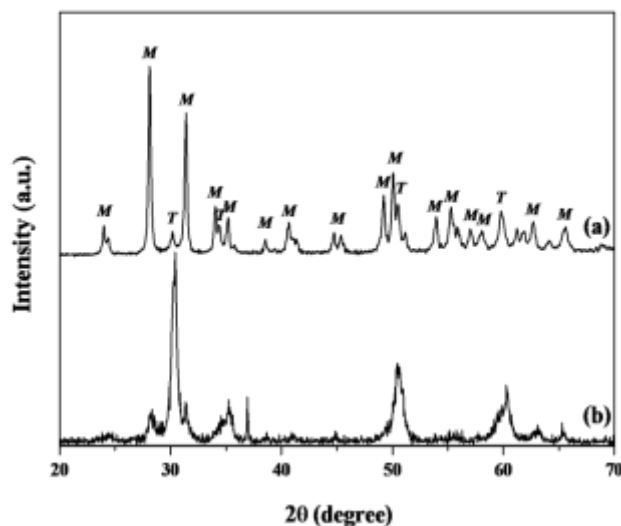


Fig. 1 XRD patterns of (a) pure and (b) Co-doped ZrO_2 nanoparticles.

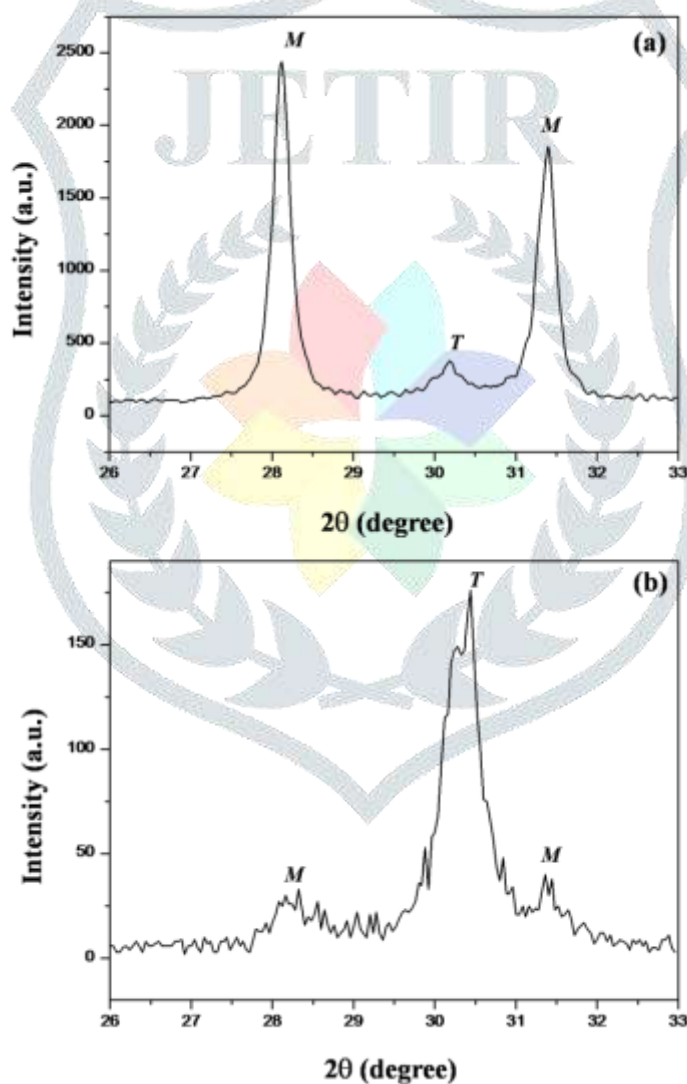


Fig. 2 Enlarged XRD patterns of monoclinic-tetragonal phase transformation of (a) pure and (b) Co-doped ZrO_2 nanoparticles.

Fig. 1(a-b) represents the powder X-ray diffraction patterns of pure and Co-doped ZrO_2 nanocrystallites, respectively. From XRD pattern (Fig.1a), it is clearly shown that the monoclinic phase in as prepared pure zirconia powder is dominant. With the addition of 1 mol% of cobalt, the monoclinic phase was suppressed and the tetragonal phase was enhanced (Fig. 1b), which due to the transformation of phase as a function of metal ion doping. This phase shifting may be attributed to the lattice mismatching, lattice distortion, strain in the crystal and finite size effect [7]. Moreover, the XRD diffraction peaks of Co-doped ZrO_2 nanoparticles decreasing intensity indicated the loss of crystallinity due to the lattice distortion by the incorporation of Co into the ZrO_2 lattice. The diffraction peaks intensity of Co doped ZrO_2 nanoparticles were observed to be lower than pure ZrO_2 nanoparticle due to Co ion incorporated into the periodic lattice of ZrO_2 , and induced the strain at the Zr sites.

The intensity of diffraction peaks of monoclinic phase was suppressed by doping of 1 mol % Co, and tetragonal phase was enhanced and the enlarged image was shown clearly in Fig.2 (a-b). This strain is alternated the lattice periodicity and decrease the crystal symmetry of Co doped ZrO₂ nanoparticles. It is clear that there are no extra peaks due to cobalt metal oxides implying that the transition metal ion get substituted at the Zr site without changing the structure. Furthermore, the crystallite size was calculated using the Scherrer formula [8],

$$D = K\lambda/\beta\cos\theta,$$

where θ is the Bragg angle and β is the full width at half maxima, $\lambda = 15405$ nm in the CuK $_{\alpha 1}$ radiation. The Co doped ZrO₂ nanoparticles was observed to be the lower crystallite size. It has also been reported that the impurities in the metal oxide nanopowders affects the nucleation and growth of nanoparticles. Therefore, the size of Co-doped ZrO₂ nanoparticles would be affected by the nucleation and growth process of ZrO₂ nanoparticles by the inclusion of Co atom in to the ZrO₂ lattice. The average crystallite size of pure and Co-doped ZrO₂ nanoparticles were calculated using scherrer's formula and were found to be 15.43 and 9.52 nm respectively.

Fig. 3 shows the FT-IR spectra of pure and Co-coped ZrO₂ samples dried at 120°C, in the 400–4000 cm⁻¹ regions. The bands located around 3400 and 1600 cm⁻¹ as stretching and bending frequencies, respectively. They are related to OH of adsorbed water and it is found that the traces of water disappeared for samples treated at elevated temperature [9]. The bands centered at 1030 and 1420 cm⁻¹ can be associated to stretching vibrations of Zr-O terminal groups. Furthermore, band at 685 cm⁻¹ that is assigned to Zr-O-Zr asymmetric mode, which confirm the formation of ZrO₂ phase [10].

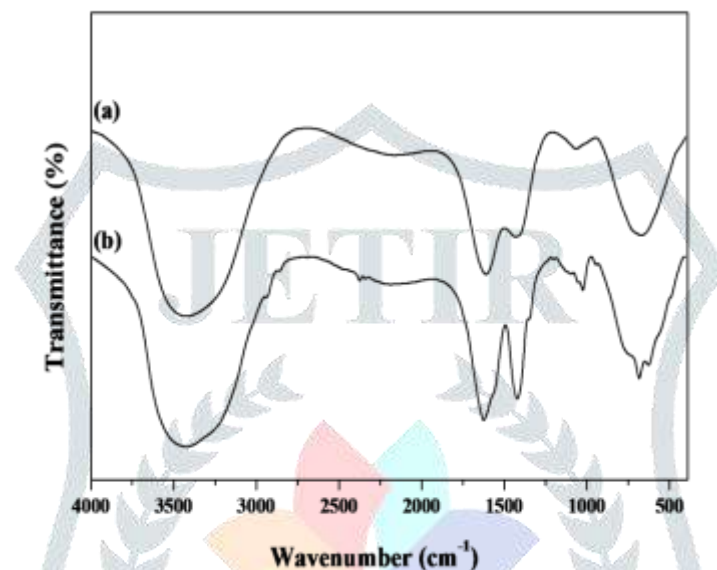


Fig. 3 FTIR spectra of (a) pure and (b) Co-doped ZrO₂ samples dried at 120°C

The UV–Visible absorption spectra of pure and Co-doped ZrO₂ nanoparticles in the wavelength range 200–800 nm was shown in Fig. 4. The spectra shows strong and prominent absorption band with maximum at around 244 nm which mainly could arise due to transition between valence band to conduction band [11], this shows the presence of oxygen vacancies in the ZrO₂ lattice. There is no other pronounced absorption peak observed in the UV-vis spectra due to no electrons found in the d-orbital of the zirconia as it is in the Zr⁺⁴ oxidation state. Hence the charge transfer transition O(2p) → Zr⁺⁴(A_{1g}). This charge transfer transition corresponds to the transfer of electron from O(2p) valence band to Zr⁺⁴ (4d) conduction band. Smaller sized particles were found to have high surface to volume ratio. This results in increase of defects distribution on the surface of nanomaterials. Thus if the particle size is small; nanomaterials exhibit strong and absorption bands [12]. In Co-doped ZrO₂, the particle size was in smaller than that of pure sample which results in high surface to volume ratio as a result; there is an increase in defects distribution on the surface of the Co-doped ZrO₂ nanoparticles.

Based on the absorption spectra, the optical band-gap was determined by using Tauc's relationship [13]:

$$\alpha h\nu = B (h\nu - E_g)^n$$

where α is the optical absorption coefficient, $E (= hc/\lambda)$ is the photon energy, B is a constant, E_g is the optical band gap and n is 1/2 or 2 for direct or indirect band gap semiconductor, respectively. E could be approximated by:

$$E = 1240/\lambda$$

where λ is the measured wavelength in nm. Tauc's plots for pure and Co-doped ZrO₂ nanoparticle samples show that band-to-band direct transitions are more likely to occur than the direct transitions. Fig. 5 shows the band energy gap was determined by plotting $(\alpha h\nu)^2$ versus $h\nu$ and finding the intercept on the 'hν' axis by extrapolating the plot to $(\alpha h\nu)^2 = 0$. The band gap (E_g) values of pure and Co-doped ZrO₂ nanoparticles were measured to be 5.23 and 5.38 eV, from which it can be seen that the E_g value for the Co-doped sample is higher than that for the pure one.

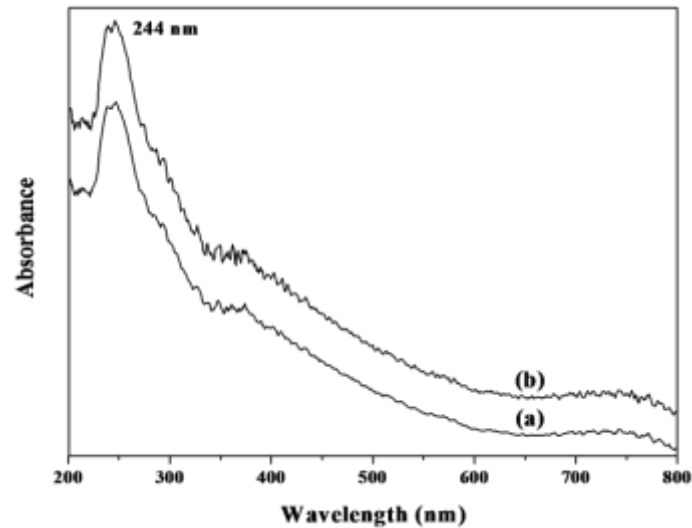


Fig. 4 UV-vis absorption spectra of (a) pure and (b) Co-doped ZrO_2 nanoparticles.

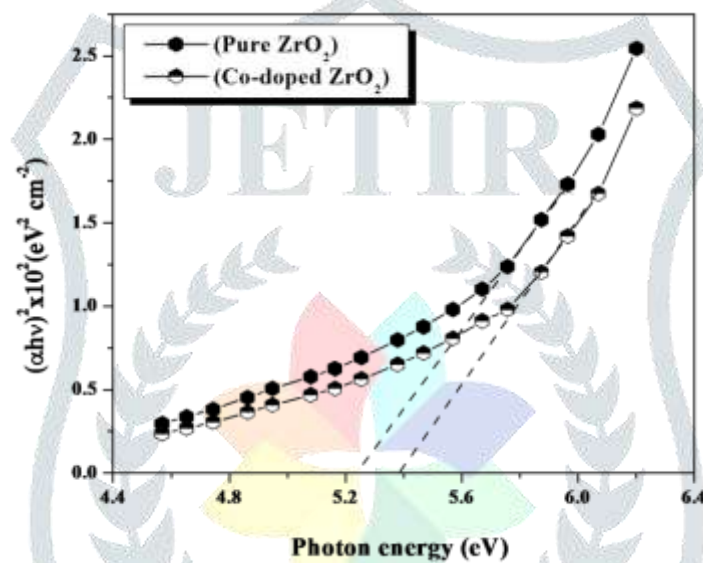


Fig. 5 $(\alpha h\nu)^2$ versus $h\nu$ spectra of (a) pure and (b) Co-doped ZrO_2 nanoparticles.

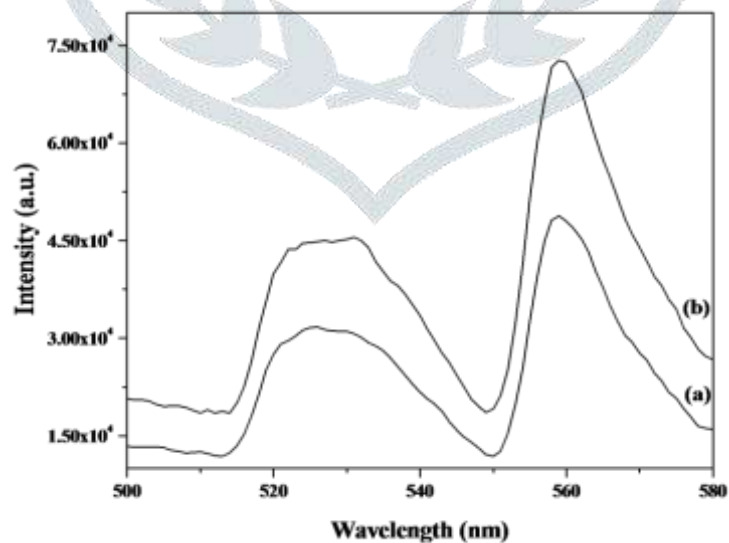


Fig. 6 Photoluminescence emission spectra of (a) pure and (b) Co-doped ZrO_2 nanoparticles.

To further investigate the effect of modification of ZrO_2 by Co doping, the photoluminescence emission spectra were recorded. Nanostructured materials have a higher density of crystalline defects, such as stacking faults, oxygen defects etc., than their bulk counterparts. In this case, the photoluminescence emission peak can be attributed to such crystal defects within the ZrO_2 matrix. The photoluminescence emission spectra of pure and Co-doped ZrO_2 nanoparticles were measured at room temperature, as shown in Fig.6. The broad and sharp emission peaks centered at 527 and 559 nm mainly arises due to the contribution of mid-gap trap states like surface defects and oxygen vacancies. The Co ion dopant influences the photoluminescence property as revealed by intensity enhancement in the emission

peak. The increase in density of oxygen vacancy due to Co ion dopant as revealed by phase transformation may be the reason behind the observed increase in PL intensity.

IV. CONCLUSION

Pure and Co-doped ZrO₂ nanoparticles were successfully prepared by the precipitation method. The XRD pattern revealed that the monoclinic phase of pure sample is transferred to tetragonal phase of ZrO₂ by the effect of Co-doping and also Co-doped ZrO₂ sample showed smaller crystallite size, which due to the lattice mismatching, lattice distortion, strain in the crystal and finite size effect. Further, the optical properties of pure and Co-doped ZrO₂ nanoparticles were studied, Co-doped ZrO₂ nanoparticles showed enhanced optical properties than that of pure one.

REFERENCES

- [1] Chen, L. Liu, Y. and Li, Y. 2004. Preparation and characterization of ZrO₂:Eu³⁺ phosphors. *Journal of Alloys and Compounds*, 381: 266-271.
- [2] Spijksma, G.I. Huisjes, C. Benes, N.E. Kruidhof, H. Blank, D.H.A. Kessler, V.G. and Bouwmeester, H.J.M. 2006. Microporous Zirconia-Titania Composite Membranes Derived from Diethanolamine-Modified Precursors. *Advanced Materials*, 18: 2165-2168.
- [3] Chandra, N. Singh, D.K. Sharma, M. Upadhyay, R.K. and Ammritphale, S.S. 2010. Synthesis and characterization of nano-sized zirconia powder synthesized by single emulsion-assisted direct precipitation. *J. Colloid Interface Sci.*, 342: 327-332.
- [4] Howard, C. J. Hill, R. J. and Reichert, B. E. 1988. Structures of ZrO₂ polymorphs at room temperature by high-resolution neutron powder diffraction. *Acta Crystallogr., Sect. B: Struct. Sci.*, 44: 116-120.
- [5] Stefanovich, E. V. Shluger, A. L. and Catlow, C. R. A. 1994. Theoretical study of the stabilization of cubic-phase ZrO₂ by impurities. *Phys. Rev. B*, 49: 1560-11570.
- [6] Stapper, G. Bernasconi, M. Nicoloso, N. and Parrinello, M. 1999. Ab initio study of structural and electronic properties of yttria-stabilized cubic zirconia. *Phys. Rev. B*, 59: 797-810.
- [7] Vidya, Y.S. Gurushantha, K. Nagabhushana, H. Sharma, S.C. Anantharaju, K.S. Shivakumara, C. Suresh, D. Nagaswarupa, H.P. Prashantha, S.C. and Anilkumar, M.R. 2015. Phase transformation of ZrO₂:Tb³⁺ nanophosphor: Color tunable photoluminescence and photocatalytic activities. *Journal of Alloys and Compounds*, 622: 86-96.
- [8] Cullity, B.D. and Stock, S.R. 2001. *Elements of X-ray diffraction*, 3rd ed., Prentice Hall, Upper Saddle river, NJ, 388.
- [9] Guo, G.Y. Chen, Y.L. and Ying, W.J. 2004. Thermal, spectroscopic and X-ray diffractational analyses of zirconium hydroxides precipitated at low pH values. *Mater. Chem. Phys.*, 84: 308-314.
- [10] Sahu, H. R. and Rao, G. R. 2000. Characterization of combustion synthesized zirconia powder by UV-vis, IR and other techniques. *Bull. Mater. Sci.*, 23(5): 349-354.
- [11] Das, S. Yang, C.Y. and Lu, C.H. 2013. Structural and Optical Properties of Tunable Warm-White Light-Emitting ZrO₂:Dy³⁺-Eu³⁺ Nanocrystals. *J. Am. Ceram. Soc.*, 96: 1602-1609.
- [12] Emeline, A. Kataeva, G.V. Litke, A.S. Rudakova, A.V. Ryabchuk, V.K. and Serpone, N. 1998. Spectroscopic and Photoluminescence Studies of a Wide Band Gap Insulating Material: Powdered and Colloidal ZrO₂ Sols. *Langmuir*, 14: 5011-5022.
- [13] Chrysicopoulou, P. Davazoglou, D. Trapalis, C. and Kordas, G. 1998. Optical properties of very thin (<100 nm) sol-gel TiO₂ films. *Thin Solid Films*, 323: 188-193.